PROC. 24th INTERNATIONAL CONFERENCE ON MICROELECTRONICS (MIEL 2004), VOL 1, NIŠ, SERBIA AND MONTENEGRO, 16-19 MAY, 2004

Power Capabilities of RF MEMS

B. Ducarouge, D. Dubuc, F. Flourens, S. Melle, E. Ongareau, K. Grenier, A. Boukabache, V. Conedera, P. Pons, E. Perret, H. Aubert, and R. Plana

Abstract – This paper outlines the power capabilities of RF MEMS devices. It is shown the specific needs concerning the technology, the design and the geometry of the devices in order to circumvent self-actuation, AC electromigration, thermal effect and Reliability.

I. INTRODUCTION

The emergence of wireless applications in various applications have resulted to new requirement for the RF and millimeterwave modules in term of microwave performances (i.e noise, linearity) in term of functionalities (reconfigurability, reparing, tunability) and in term of cost, volume and weight. It has been observed that conventionnal Integrated Circuit technologies were not able to afford all these new requirements and this has motivated the explosion of a new type of technology based on the joined exploitation of the mechanical and electrical properties called MicroElectromechanical Systems (MEMS). A lot of efforts have been conducted in this field and some very attractive building blocks are emerging as switches [1-6], tunable filters [7,8], reconfigurable antennas [9] redundancy ring [10] and phase shifters [11,12]. Nevertheless some issues are still under discussion as the reliability behavior of the MEMS based devices where only very few results are reported [13, 14] as well as their power capabilities [15, 16, 17] where there is a lack of data concerning the self actuation, the electromigration, the design methodology that has to include coupling between mechanical, thermal and electromagnetic properties. Power capabilities of RF MEMS are one of the major issue for the future as it is seen very attractive applications for smart power amplifier optimization, for space applications (reconfigurable antenna and filter for emitter path). In this paper we will outline the power capabilities of RF MEMS. Section II will briefly describe some major issues that have to be circumvent (self-actuation, electromigration..). Section III will address the design methodology that is preconized when Section IV will give some details concerning the technological process and will report some results already obtained with some reliability properties. Conclusions will be detailed in section V.

B.Ducarouge, D.Dubuc, S.Melle, A.Boukabache, K.Grenier, F.Flourens, V.Conedera, P.Pons, and R.Plana are with LAAS – CNRS, France, E-mail: plana@laas.fr

X.Chauffleur is with Epsilon Engineerie, France.

E.Ongareau is with MBDA, France.

E.Perret and H.Aubert are with Len7, France.

II. SELF-ACTUATION AND ELECTROMIGRATION

It has been already discussed that the best trade off for the actuation of moveable membrane is the electrostatic actuation. It combines simplicity of fabrication, a high actuation speed and a near zero power consumption and today almost all the RF MEMS devices exhibit this actuation method even, if we report some isolated results concerning thermal actuation and magnetic actuation. This actuation method of course exhibits some drawback as dielectric charging [16, 17], and self actuation due to high power.

It is understood that the DC actuation voltage of a bridge can approximated by the following equation:

$$Vp = \sqrt{\frac{8kg_o^3}{27\varepsilon_o A}} \tag{1}$$

where k represents the stiffness of the bridge in the moving direction, go is the initial height of the bridge, A is the actuation area which sometimes is the switch area where the electrostatic force is applied and εo represents the free space dielectric permittivity.

If an RF signal featuring a magnitude Vo is applied it generates an equivalent DC voltage through the following equation.

$$Veq = \frac{Vo}{\sqrt{2}} \tag{2}$$

Considering the equation (2), we can calculate the equivalent input power through the equation (3).

$$Pin = \frac{Vo^2}{2Zo} \tag{3}$$

Considering the equations (1-3), it is obvious that the equivalent DC voltage could produce a self actuation mechanism if it is larger than the acdtuation voltage given in equation (1). In figure 1, we have plotted the evolution of the equivalent actuation voltage versus the RF input power for two characteristic impedance.

We can see on the curves that if a switch exhibits an actuation voltage of 22 volts it will handle a maximum power of 10 watts when a switch featuring a 50 volts acuation voltage handles a RF power of 50 watts. Asumming this results it appears that it is important to decouple the actuation area and the RF parts where the signal will circulate.

0-7803-8166-1/04/$17.00 © 2004 IEEE

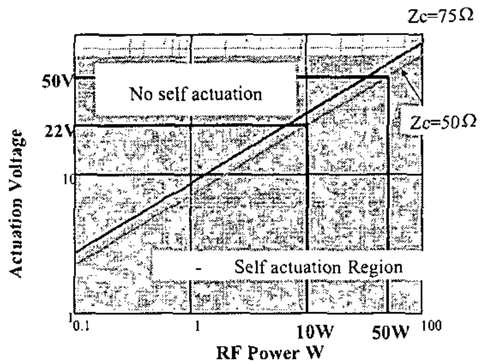

Fig. 1. Actuation voltage evolution versus RF Power for two characteristic impedance.

Another issue deals with the high current that propagates within the transmission lines and within the upper membrane. It is well known that the current lines can generate electromigration effect that degrades the conductivity of the metallization leading to an increase of the temperature through a rise of the ohmic losses. Of course in RF the electromigration impact is not similar than the impact in DC. It has been already demonstrated that due to skin effect when the operating frequency is increasing this in turns to a higher concentration of the current lines. It has been also shown that in RF the electromigration limit is pushed out to higher current density [18]. We have conducted DC life test on coplanar wave guide featuring electrolitic gold metallization. The line has failed for a DC current density of 6GA/m^2. Figure 2 shows the degradation mechanism wiht a breakdown of the center conductor.

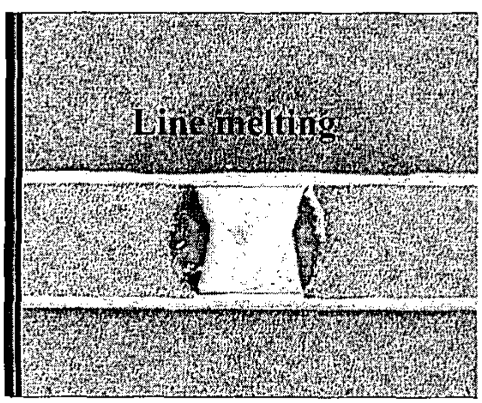

Fig. 2. Failure signature after a DC life test experiments.

Other experiments have been done on coplanar wave guide with a RF power at 18 GHz. The results are summarized in table I.

TABLE I.
AC LIFE TEST AND COMPARISON BETWEEN DC AND AC LIFE TESTS EXPERIMENTS

Power Max@ 18 GHz	J_{MAX} (GA/m^2)	J_{MAX_RF} / J_{MAX_DC}
17,8 W	185	37
20 W	196	39
22,4 W	207	41

The results show that in AC regime the maximum current density leading to the line failure is 30 times higher than the maximum current density observed in DC regime which means that the mean time to failure through RF stress will be 1000 (J^2) higher than the mean time to failure through DC stress.

III. Design Methodology

The proposed topology for the high power MEMS switch is presented in figure 3. It is composed of a capacitive shunt bridge realized on a CPW line with two specific issues: (1) the switch is isolated from the CPW line and (2) the attracting electrodes are located on the CPW ground planes.

The design of such non-uniform width structure consists in making independent the optimizations of electrostatic (the actuation voltage), mechanical (the stiffness) and electromagnetic (the equivalent capacitor) performances. Indeed, on the one hand, the widths We and Wm (see figure 3) respectively control the stiffness and the pull down voltage. On the other hand, the insertion loss and the isolation of the RF MEMS switch are fixed by the width Wμ.

The concept of an isolated bridge translates into two interests: (1) the possible design of capacitive serial switches and (2) the simplicity of the attracting electrodes formed by the CPW ground planes.

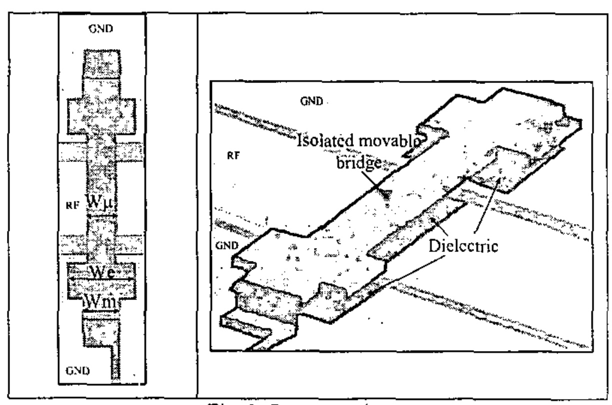

Fig. 3. Structure views.

This structure has been optimized using COVENTORWARE software and the results are: a pull down voltage of 30 V and a stiffness of 5 N/m.

In order to design and optimize more complex passive circuits, electrical models of switches are necessary. In figure 4, we have developped a scalable equivalent electrical model from electromagnetic simulations (Sonnet) that allows a very fast optimization of the microwave performances.

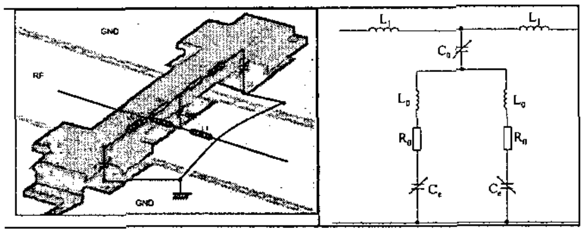

Fig. 4. Electrical model topology of the high power MEMS switch

It has been developed a devoted electromagnetic design methodology to evaluate the current density in the structure and warrants that the electromigration threshold or the maximum temperature are not achieved.

1. Approximation of the current density and the dissipated power density in a conductor-backed coplanar waveguide

The figure 5 shows the cross-sectional view of the studied conductor-backed coplanar waveguide (CPWG). Moreover we consider a finite conductivity σ only for the CPWG discontinuity plane.

The characteristic impedance Z_C is known (Z_C is close to 70Ω for the dimensions given in figure 5).

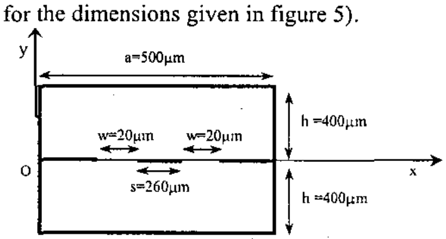

Fig. 5. Cross-sectional view of the studied CPWG.

The thickness t of the CPWG is large compared to the skin depth δ (in practice t = 3μm, and consequently, at 30GHz, the thickness is close to 10δ for CPWG manufactured in copper). Consequently, a surface impedance model can be advantageously used for taking into account the ohmic losses in the waveguiding structure. The dissipated power density in the CPWG is then approximated by $\frac{1}{2} Z_S J^2$ where J is the current density in the lossless case and, Z_S ($Z_S=1/\sigma\delta$) is the surface impedance.

The current density J is deduced from the Transverse Resonance Method. Since the width w of the slit is small compared to a, we adopt only one trial function for the representation of the electric field in the discontinuity plane. The current density J for y=0 is then given by the following analytical expression:

$$J(x)=\frac{2\sqrt{2Z_cP_{EM}}}{Z_0\,a} \tag{4}$$
$$\times \sum_{n=0,1,2,3..} (-1)^n .\coth\left[(2n+1)\pi\frac{h}{a}\right].\sin\left[(2n+1)\frac{\pi}{2}\frac{s+w}{a}\right].J_0\left[(2n+1)\frac{\pi}{2}\frac{w}{a}\right].\sin\left[(2n+1)\frac{\pi}{a}x\right]$$

where P_{EM} is the electromagnetic power carrying by the TEM-mode along the CPWG (by assumption, the only one to propagate), Z_0 designates the free-space wave impedance ($Z_0=120\pi$) and J_0 represents the first kind and zeroth order Bessel function.

The current density J' for x = (a-s)/2 - w and $y\in[-t/2,0[$ is given by [5]:

$$J'(y)=\frac{2\sqrt{2\,Z_c\,P_{EM}}}{Z_0\,w}\left\{\sum_{n=1,2,3...}(-1)^n\,J_0(n\pi)\,\frac{ch\left[2n\frac{\pi}{w}\left(\frac{t}{2}+y\right)\right]}{ch\left(n\pi\frac{t}{w}\right)}\right\}. \tag{5}$$

where ch(x) designates the hyperbolic cosine of x.

For P_{EM} = 10W (carrying by the TEM-mode), the figures 6 and 7 display the dissipated power densities p_d and p'_d respectively. 2500 tones are used to compute p_d while 500 tones allows to reach the convergence for p'_d.

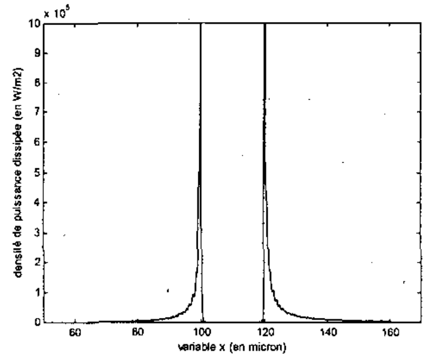

Fig. 6. Dissipated power density p_d in the discontinuity plane of the CPWG shown in figure 5.

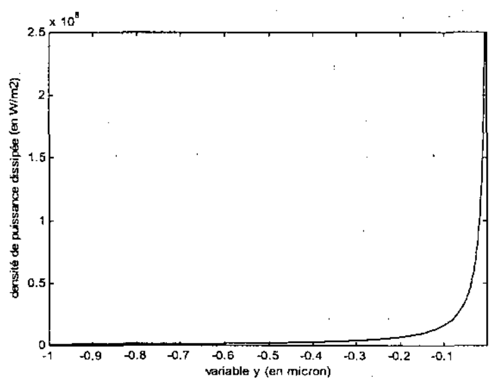

Fig. 7. Dissipated power density p'_d in the slit of the CPWG shown in figure 3.

From the current density, the electromigration phenomenon can be minimize through the suitable design of the line (see the following section) as from the dissipated power density, the temperature profile can be determined.

Electromigration occurs under high current densities: atoms of conductive material are lifted by the current leading to open circuit failures. The critical current density above which electromigration effect happens is about J_{max}=1 MA / cm^2 in gold.

The previously presented method, associated with E.M. simulations (ANSOFT HFSS) in which the conductors have been meshed in volume, are used to estimate the maximum current density handled by 50 ohms coplanar and microstrip lines.

Maximum current densities of coplanar lines (made on a 20 µm thick BCB interlayer above silicon substrate) for different conductor and gap widths (resp. S and W) have been simulated. Microstrip lines on a 10 or 20 µm BCB layer (W: conductor width and t: BCB layer thickness) have also been evaluated. The maximum handling power depends on the specific incident power used for simulation: P_{SIMU}, the maximum current density simulated: J_{SIMU} and the electromigration threshold: J_{MAX}, according to:

$$P_{MAX}=P_{SIMU}\cdot\left(\frac{J_{MAX}}{J_{SIMU}}\right)^2 \qquad (6)$$

TABLE II.
MAXIMUM POWER HANDLED BY CPW AND MICROSTRIP LINES

Lines	microstrip		CPW		
Dimensions (µm)	**S=25 t=10**	**S=50 t=20**	**S=90 W=10**	**S=180 W=50**	**S=250 W=100**
Zc (Ohm)	50	50	52	50	48
Max power @ 10 GHz	**0.7 W**	**2.5 W**	**9 W**	**22 W**	**32 W**
Max power @ 20 GHz	**0.4 W**	**1.3 W**	**5 W**	**12 W**	**17 W**

The maximum powers for the different lines are reported in table 2. For this technology, wide coplanar lines are more suitable than microstrip ones for high power capabilities. Moreover, for a 30 W power handling application, coplanar line must exhibits a 250 µm central conductor width.

After this transmission line scaling, the following step addresses the design of a high power capabilities switch.

Figure 7 gives the simulated current density (using SONNET software) of the MEMS bridge realized on the previously investigated line (S=250 W=100 µm) at down state for an incident power of 1 W at 20 GHz. It is worth noticing that the current density concentrates in the bridge edge (along 20 µm) on the CPW gaps. The maximum current density (5500 A/m) is close to the electromigration threshold at 20 GHz (5800 A/m) which limits the handling power to about 1.1 W. Further investigations on the bridge design are in progress to improve its power capability.

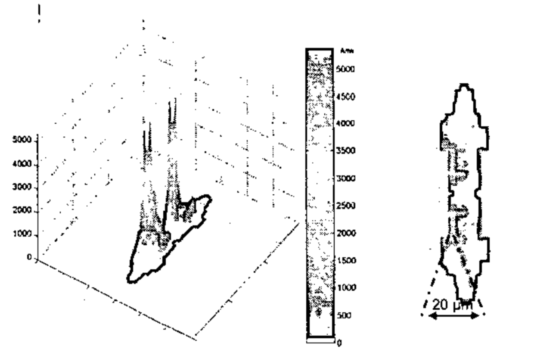

Fig. 8. Current density in power switch.

According to the results on power density, a thermal model of a CPW line has been performed using REBECA-3D software based on BEM and developed by EPSILON Ingénierie [7].

The CPW line is assumed to be realized on a two-layer membrane (2000x1300µm) as given in figure 8.

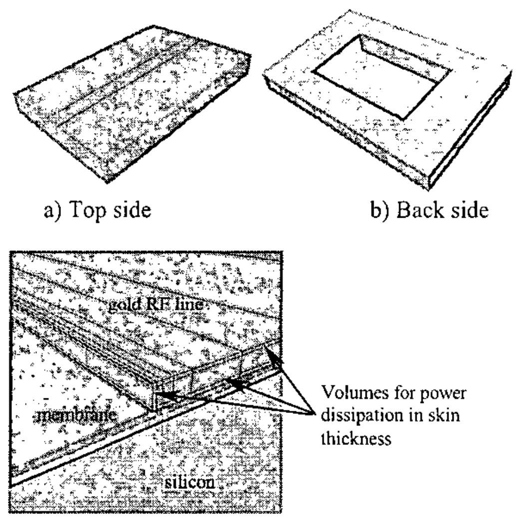

a) Top side

b) Back side

c) Close view of a "coplanar gap"

Fig. 9. Thermal model.

Power dissipation distribution along width of the RF device is redistributed as volumic power density in individual skin volume and power dissipation distribution along height of the "coplanar gap" is applied directly as flux power density (figure 9-c).

Back side of silicon is assumed to be at uniform temperature of 25°C and only conductive heat exchange is considered (no convection).

The figure 10 shows that the maximum temperature is located on the line and is of 56.5°C which means a rise of 31.5°C. Moreover, one notes that the part on the membrane is definitely hotter because of the strong thermal resistance of the latter.

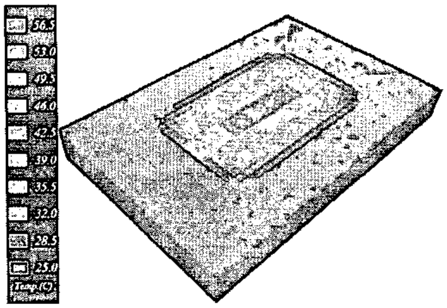

Fig. 10. Temperature distribution.

Even if this rise is weak, mechanical study will be undertaken to check if the thermo-mechanical stresses are not sufficient to cause the buckling of the membrane in spite of its pre-tensioning.

These thermal studies outline that the temperature rise of the coplanar line doesn't translate into thermal failures. Similar studies on MEMS bridges are under investigation.

After the development of the design methodology, we have proposed a devoted topology of switch that is able to circumvent both the electromigration and the self actuation problems. More precisely, we have chosen a double electrodes Topology in order To suppress the self actuation effect. DC electrodes are separated from the RF signal to limitate the DC electromigration influence on the microwave characteristics, the dielectric charging and to simplify the design flow as both quantities are almost independant and then can be adjusted separately. This topology is presented in figure 11.

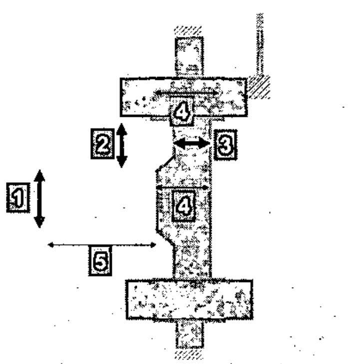

Fig. 11. Topology of power switch.

In table 2, we have calculated the influence of the different region of the switch with respect to the reliability and the electrical performance.

Using this methodology and the topology, we have designed the switch for broadband range power applications. Figure 12 shows the results of the insertion that has been obtained.

TABLE III.
SENSITIVITY OF THE SWITCH REGION WITH RESPECT TO THE ELECTRICAL AND RELIABILITY PERFORMANCES

	J CPW	J bridge	Isolation	Loss
1	X	X	X	X
2	X	X	X	X
3		X	X	
4		X	X	
5				X

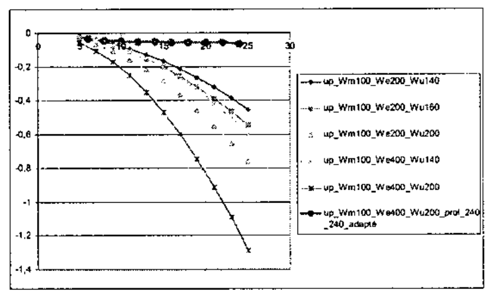

Fig. 12. Insertion loss simulation for the optimized power switch.

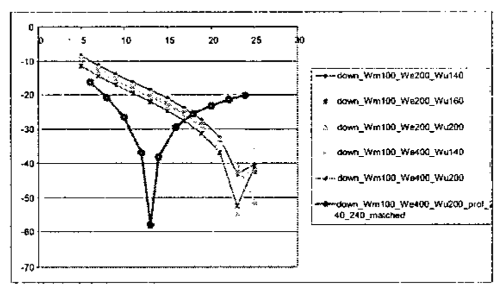

Fig. 13. Isolation simulation for the optimized power switch.

The results indicate that it is possible to have a very high isolation and low loss with the topology that has been proposed. Actually, the expected results are 0.06 dB insertion loss up to 20 GHz, isolation of -16 dB on a very broad band range (6-18 GHz) and power handling of 3.8 W at 20 GHz.

III. TECHNOLOGY AND PRELIMINARY RESULTS

The technological process of this structure uses surface micromachining to realize air-gap bridges.

First of all, a BCB layer is deposited on a HRS silicon substrate. Then are processed the gold coplanar line on top. An isolation dielectric layer between the line conductor and the bridge is patterned to avoid the stiction of the bridge when it is down.

The elaboration of the air-gap bridges begins with the patterning of a sacrificial photoresist to fix the anchorages. A thin seed metallic gold layer is evaporated on the photoresist and then gold is electroplated. After gold patterning, the sacrificial layer is etched by solvents.

As we have chosen a double electrodes topology as plotted in figure 14, it has been necessary to developp a devoted process for multi level sacrificial layer that has been done using BCB materials.

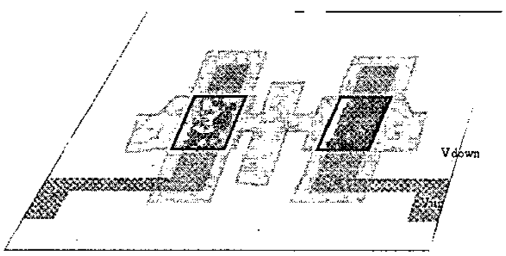

Fig. 14. View of the double electrode power switch.

The structures have been fabricated and they feature insertion loss in the 0.2 dB range with isolation in the -10 dB range due to a roughness problem and some problems concerning the flatness of the bridge. More details will be given at the conference.

We also have conducted some reliability investigation using a specific test set that has been developped in house. It has been shown that the main reliability issue was still associated with dielectric charging has we have observed a drift of the actuation voltages. More details will be given at the conference.

III. Conclusion

This paper reports on the power capabilities of the RF MEMS. We have shown that dedicated characterization and modelling methods was preconized to have a clear view of the AC electromigration, the self-actuation and the microwave performance. Using a specific methodology, we have proposed an original toplogy of switch handling 3.8W at 20 GHz. Finally, the technology has been developped and the preliminary results are very attractive. More results will be presented at the conference as a lot of measurements are in progress.

References

[1] R.E.Mihailovich et al., "MEM relay for reconfigurable RF Circuits", IEEE Microwave Wireless Comp Lett, vol 11, pp 53-55, 2001.

[2] D.Hyman et al., "Surface Micromachined RF MEMS switches on GaAs susbtrates", Int Journal RF Microwave Computer Aided Engineering, vol 9, pp 348-361, Aug 1999.

[3] S.Duffy et al., "MEMS microswitches reconfigurable microwave circuitry", IEEE Microwave Wireless Comp Lett, vol 11, pp 106-108, March 2001.

[4] P.M.Zavracky et al., "Microswitches and microrelays with a view toward microwave applications", Int. Journal RF Microwave Comp Aided Engineering, vol 9, pp 338-347, July 1999.

[5] C.L.Goldsmith et al., "Performance of low loss RF MEMS capacitive switches", IEEE Microwave Guided Wave Letter, vol 8, pp 269-271, Aug 1998.

[6] K.Grenier, P.Pons, R.Plana, J.Graffeuil, "Bulk silicon micro-machined MEM switches for millimeter-wave applications" 31st European Microwave Conference, Londre (GB), 24-28 Septembre 2001, 3p.

[7] D.Peroulis et al., "Tunable lumped components with applications to reconfigurable MEMS filters", in IEEE MTT-S Int Microwave Symp, vol 1, pp 341-344, May 2001.

[8] C.Bozler et al., "MEMS microswitch arrays for reconfigurable distributed microwave components", in IEEE MTT-S, Int Micrawave Symp, vol 1, pp 153-156, June 2001.

[9] J.C.Chiao et al "MEMS reconfigurable antenna" in IEEE MTT-S Int Microwave Symp, vol 2, pp 1515-1518, June 1999.

[10] D.Dubuc, L.Rabbia, K.Grenier, P.Pons, O.Vendier, J.Graffeuil, R.Plana, "Original MEMS-based single pole double throw topology for millimeter wave space communications", 33rd European Microwave Conference (EuMC'2003), Munich (Allemagne), 6-10 October 2003, pp.979-982.

[11] N.S.Barker and G.M.Rebeiz "Optimization of distributed MEMS transmission line phase shifters U-Band and W-Band" IEEE Trans on Microwave Theory, vol 48, pp 1957-1966, Nov. 2000.

[12] J.S.Hayden and G.M.Rebeiz "Low loss cascadable MEMS distributed X-Band phase shifters" IEEE Microwave and Guided Wave Lett, vol 10, pp 142-144, Apr 2000.

[13] C.Goldsmith et al "Lifetime characterization of capacitive switches", in IEEE MTT-S Int Microwave Symp, vol 1, pp 227-230, June 2000.

[14] S.Melle et al., "Investigation of dielectric degradation of microwave capacitive microswitches", MEMS 2004 Symposium, Maastricht, pp 141-144.

[15] W Thiel et al., "A study of thermal effects in RF MEMS switches using a time domain approach", in IEEE MTT-S Int Microwave Symp, vol 1, pp 235-238, June 2001.

[16] J.Risk et al "Steady state thermal analysis and high power reliability considerations of RF MEMS capacitive switches" in IEEE MTT-S Int Microwave Symp, vol 1, June 2002, pp 239-242.

[17] B.Ducarouge et al., "Design of MEMS-based microwave and millimeterwave switches for high power applications", 26th IEEE International Semiconductor Conference (CAS'2003), Sinaia (Roumanie), 28 Septembre - 2 Octobre 2003, pp.61-64.

[18] J.Tao et al., "An electromigration Failure Model for interconnects under pulsed and bidirectional current stressing" IEEE Electron devices, vol 41, n°4, pp 539-545, April 1994.

[19] REBECA-3D : http://www.rebeca3d.com